Absorbing boundaries in time-dependent problems with discretized energy continua

M. G. Makris*
Department of Physics, University of Crete, P.O. Box 2208, Heraklion 711 10, Greece
(Received 16 December 2003; published 15 June 2004)

We develop a general method for removing artifacts associated with the numerical solution of time-dependent Schrödinger equation (TDSE) involving a (multiple) energy continuum discretization. This method is the equivalent to absorbing boundaries in the case where the space is discretized. By removing the reflected part of the wave function (on the artificial boundaries of the system), one is able to reduce the computational cost of the calculations, with a benefit scaling as the power of the continuum multiplicity. As a demonstration, we apply our method to the TDSE of a hydrogen atom subjected to a laser pulse, the spontaneous emission of a two-level atom in free space, and the interaction of two photons with a two-level atom and a defect mode at the edge of a photonic band gap.

DOI: 10.1103/PhysRevE.69.066702 PACS number(s): 02.70.Hm, 32.80.−t, 42.50.−p

I. INTRODUCTION

The numerical solution of a problem that involves a continuous variable (be it energy, position, etc.) inevitably is associated with some sort of discretization. A well-studied example of this is the solution of the time-dependent Schrödinger equation (TDSE) for one (active) electron subject to an electromagnetic pulse. In this case, one can expand the electron wave function on the basis of the eigenstates of the free atom and solve the resulting system of differential equations for the coefficients of the eigenstates [1], which inevitably involves a truncation of the basis (maximum E) and a discretization of the one-electron continuum. Alternatively one can solve the Schrödinger equation directly in space, in which case the wave function is computed at a sequence of grid points [2]. In that case we also have discretization of position and truncation of the bases (maximum R).

Needless to say, the limitations we have to impose in order to describe the system can lead to artifacts on the calculated physical quantities, on top of resolution problems. In our example above, limiting the maximum radius of the discretization is equivalent to confining the atom to a sphere of radius R, with a potential that is infinite at the surface of the sphere. This means that the wave packet of the electron ejected from the atom by the radiation, after some time ($t \sim R/\sqrt{E}$), will arrive at the boundary of the sphere and will be reflected by the infinite potential barrier. Once this reflected wave packet approaches the atom, artifacts of the calculation will emerge (e.g., distorted harmonics and photoelectron spectra).

This difficulty can be circumvented by removing the wave packet that is escaping the atom (better: the nucleus), since this part of the wave function is far enough to be equivalent, in its evolution, to a free electron which does not interact with light and does not influence the atom-light dynamics. This technique has been employed with success either by employing an imaginary potential to imitate absorption [2] or by continuously multiplying the wave function with a function that goes smoothly to zero at the boundary [3] for distances higher than a certain radius, but only for the case where the wave function is computed at a sequence of grid points.

In this respect, methods based on energy discretization have an inherent drawback. The only way to get rid of these artifacts of the solution was to increase the density of the discretization, equivalent to employing a larger box, until the wave packet has not sufficient time to reflect and reinteract with the nucleus. This means that the appropriate size of the basis becomes (approximately) proportional to the time interval of the calculations. The latter is a severe limitation, especially for problems involving multiple continua, since the basis size increases as a power of the continuum multiplicity.

Another way around this problem is the addition of a small imaginary part in the eigenenergies of the continuum through complex rotation, in order to cause attenuation of the amplitudes in time. During the time they need to reflect and reinteract they are practically eliminated. This approach has been followed in a number of cases over the last two decades (among others, [4–13]). In the following, we present our contribution in constructing absorbing boundaries (AB's) for spectral methods, following a different path.

We first apply our technique to the TDSE of a hydrogen atom exposed to an electromagnetic field. This is a test ground well studied by standard techniques, where we compare our results on ionization yield, harmonic generation, and photoelectron spectra. Then we present a generalization, appropriate to handling the general class of problems involving time-dependent calculations with a discretized (energy) continuum (a) where the actual form of the wave function (or of other physical quantitities discretized, like the electromagnetic field, for example) need not be known. In this case, we show that the sole knowledge of the discretization spectrum is enough to create the necessary AB linear transformation, so the requirements for the method applicability are minimized. This generalized version is applied in the spontaneous emission of a two-level atom (TLA) in free space and in the interaction of two photons with a two-level atom

*Electronic address: makris@physics.uoc.gr

and a defect mode at the edge of a photonic band gap (PBG). We show also that one can modify the set of differential equations describing the system in a way that the AB is an inherent feature. In all cases we present, there is a substantial computational benefit since the size of the basis we have to use is smaller.

II. AB's IN THE TDSE FOR AN ATOMIC SYSTEM

A. Theory

The TDSE, in the single active electron approximation, is solved by expanding the electron wave function on a finite basis as

$$|\Psi(t)\rangle = \sum_{n=1}^{N} a_n(t)|\phi_n\rangle, \tag{1}$$

where N is the number of basis states. The choice of basis states depends on the problem at hand and our capabilities. We took the $|\phi_n\rangle$ to be the eigenstates of the atomic Hamiltonian inside a box of radius R, subject to the boundary conditions $\phi_n(0)=\phi_n(R)=0$. What is important about the basis functions we employ is their completeness (energy truncated). It is more transparent though if the basis states $|\phi_n\rangle$ are eigenstates of the atomic Hamiltonian. The TDSE is then written as a set of coupled ordinary differential equations:

$$i\dot{\vec{a}}(t) = \hat{H}\vec{a}(t), \tag{2}$$

where naturally $\vec{a}(t)=(a_1, a_2, \ldots, a_N)$ is the state vector of the system and $\hat{H}$ is the Hamiltonian matrix expressed on our finite basis.

As we discussed before, the inevitable discretization of the continuum is associated with the reflection of the wave packet at the boundaries of the box. Although in the approach we follow the spatial extent of the box is well defined by construction, we argue that one can calculate the effective energy-dependent box width where the system is limited due to the energy discretization in an exact and simple way, which depends only on the spectrum of the discretization. We discuss in more detail this issue in the following section.

In a similar way with the techniques followed in the solution of the TDSE in a lattice, we intend to multiply the wave function with a mask function $\mathcal{M}(r)$ that smoothly goes to zero when it approaches the boundaries of the box [14]. The implementation of this into atomic eigenstate expansions is not obvious due to their delocalized nature. A continumm eigenstate spans all space inside the box. Nevertheless, a superposition of the eigenstates can be well localized in space. Actually we can form a wave function well localized in a region of our choice by using a correct superposition of the eigenstates, with a localization extent in accordance with the uncertainty principle. In this spirit, we can remove the part of the state vector $\vec{a}(t)$ that corresponds to the part of the wave function of the system that approaches the boundaries. This is accomplished by a simple linear nonunitary tranform of $\vec{a}(t)$, which is constructed as follows.

Since the set of $|\phi_n\rangle$ constitutes a complete basis, we can express the action of $\mathcal{M}(r)$ on an eigenstate as

$$\mathcal{M}|\phi_n\rangle = \sum_{m=1}^{N} \mathcal{B}_{nm}|\phi_m\rangle, \tag{3}$$

$$\mathcal{B}_{nm} = \int_0^R \phi_m(r)\mathcal{M}(r)\phi_n(r)dr, \tag{4}$$

where $\mathcal{B}_{nm}$ are the elements of the $\mathcal{B}$ matrix that represents the necessary linear transformation on the basis of the eigenstates. In the present case, due to the simple boundary conditions that *a priori* define an energy-independent box width, the $\mathcal{B}_{nm}$ can be evaluated since the limits of the integral of Eq. (4) are well defined. However, in the general case, where, for example, more complicated boundary conditions are employed or where the discretized continuum spectrum is chosen by hand, this does not hold. It is not even clear if this approach has meaning, since the eigenstates can have an energy-dependent extent. This general case is handled in the next section, where we calculate $\mathcal{B}_{nm}$ based only on the discretization spectrum.

The summation is truncated to the Nth eigenstate, since we kept only the first N for our state vector of the system. One expects that this truncation would effect the $\mathcal{B}$ matrix, which is true only for the few last eigenstates, which should not play any important role in the dynamics of the system. If the latter argument is not true, the energy range has to be expanded in order to be an adequate representation of the dynamics of the system anyway.

We are able to remove the wave packet only when it approaches the boundaries since the result of the transformation on the state vector of the system depends heavily on the state vector. If the later represents a wave function localized close to the origin, it remains unaltered, while in the case that it represents a wave function localized close to the boundaries the latter is strongly attenuated. Since the transformation is linear, a wave function which has important values everywhere inside the box remains unaltered up to a chosen radius R_m and attenuated smoothly thereafter. So a frequent enough application of this transformation on the state vector during the solution of the TDSE removes the part of the wave function close to the box edge.

We calculated the $\mathcal{B}$ matrix analytically for the case of a free particle inside a box by employing a simple analytic form for the mask function (inverted Gaussian centered at the box end), obtaining rather complicated expressions. We do not present our results on this simple yet instructive problem, but we show our results on a more interesting problem, the realistic three-dimensional (3D) solution of the TDSE for a H atom subject to an intense laser pulse.

B. Application to the H atom

1. Case particulars

Our group has already used B-splines as a tool to represent atomic eigenstates for a number of years and our first example continues along these lines. As explained in more detail elsewhere [15–17], the radial part of the eigenfunc-

tions of the electron can be expressed on a B-spline basis of kth order inside a sphere ("box") of radius R, the nth radial eigenfunction being

$$P_n(r) = \sum_i c_{in} B_i(r), \tag{5}$$

subject to the typical fixed boundary condition $P_n(0) = P_n(R) = 0$. We followed a slightly different approach for the calculation of the matrix elements $\mathcal{B}_{nm}$ in order to take full advantage of the nature of B-splines. This way, the calculations are done in a faster and simpler way, leading to similar result.

We represent the $\mathcal{M}$ operator on the B-spline basis as a diagonal matrix, the elements of which are equal to 1 up to the (m,m) element and smoothly go to zero onward, with R_m being the grid point where the attenuation of the wave function starts. Since B-splines partially overlap in space, this leads effectively to a moving average of the mask function on the grid, with window size analogous to the order of B-splines we use. Since the mask function has to be a smooth function, this averaging causes minimal and insignificant changes. Nevertheless, if one wishes to have absolute control of the form of $\mathcal{M}$ operator in space, this approximation can be lifted by constructing the $\mathcal{M}$ matrix with the last part (the block $\mathcal{M}_{ij}$ with $i,j \geqslant m$) being a banded with a width equal to the order of the B-splines we use—i.e., the number of B-splines that overlap in any internal grid point.

Then the matrix elements $\mathcal{B}_{nm}$ have to be calculated by means of

$$\mathcal{B}_{nm} = \int_0^R \left(\sum_{j=1}^N c_{jm} B_j(r) \right) \left(\sum_{i=1}^N \mathcal{M}_{ii} c_{in} B_i(r) \right) dr, \tag{6}$$

limited due to the localized nature of B-splines to $|i-j| \leqslant k/2$.

Still, there is an even simpler approach in this particular case. If C is the matrix of the coefficients c_{ij}, then $C\vec{a}$ gives the weight of the B-splines for the full wave function. Then, we can smoothly remove the last ones and perform the inverse transformation C^{-1} to obtain the new state vector. In this language $\mathcal{B} = C^{-1}\mathcal{M}C$ is a linear transformation that results in a new state vector which stands for a new wave function unaltered in the region $0 < r < R_m$ and smoothly attenuated to 0 in the region $R_m < r < R$.

Once the $\mathcal{B}$ matrix is calculated, one way or another, the application of AB's to the TDSE is simply a matter of vector-matrix multiplication. In practice, the electron wave function is the sum of the partial wave functions for each l. Since for every l we have a different set of eigenstates, a different $\mathcal{B}$ matrix has to be calculated for every l and applied only to the eigenstate coefficient of this specific l. One should also note that the frequency of the application of the AB's on the coefficients depends on the mask width and on the fastest wave packet we want to absorb. A wave packet with average velocity v would stay inside the absorbing boundary for a time interval $2(R-R_m)/v$, in which time it should attenuate, so the absorbing boundary should be applied enough times in the meantime.

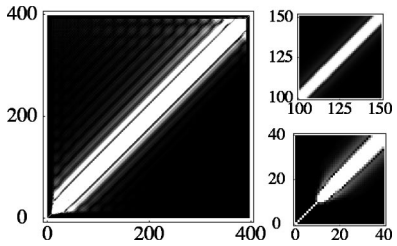

FIG. 1. The absolute value of the absorbing boundary matrix calculated for a hydrogen atom in a box of 400 a.u. using 400 B-splines on a uniform knot sequence, resulting in approximately 400 eigenstates (for $l=0$). The smaller plots on the right are magnified parts of the same matrix. The brighter the color, the higher the value of the matrix element.

One advantage of the AB's in a spectral method, in the way we formulate them, over their lattice analog, is that since the coefficients of all eigenstates included in the solution of the TDSE are known in every step, it is a easy task to keep track of the population changes after the application of the absorbing boundary matrix. This provides additional information that energetically characterizes the part of the wave function that is absorbed or removed. Following this idea, we sum for every eigenstate the population change occurring in every mask application. If one wishes to calculate the photoelectron spectrum (PES), the population of every eigenstate that has remained (i.e., not absorbed) can be added to the total population removed from this eigenstate by absorption. In general, a similar method can be followed to reconstruct energy resolved quantities for the problem at hand.

2. Results

For our calculations we have used the hydrogen atom inside a box of $R=400$ a.u. using 400 B-splines. Since we used fixed boundary conditions, this results in about 400 discrete eigenstates of the system. The calculation of the absorbing boundary matrix is straightforward and the result is presented in Fig. 1 (S symmetry). It is evident that the elements of the matrix take important values close to its diagonal. The typical width of the distribution of the weights is related to the width of the mask function. Steeper mask functions result in a broader distribution to provide the required bandwidth. Actually, the matrix elements oscillate, which is better shown in Fig. 2 where the coefficients and not their absolute value are given. This is natural, since the result of the absorbing boundary matrix on the state vector should be sensitive on the relative phase (sign) of its coefficients, as explained in more detail in the following section (Sec. III).

The first eigenstates of the system are of course the bound ones. A part of the matrix in the region of the bound states is shown at the right bottom part of Fig. 1. For the first bound states the matrix is practically identical to a unitary matrix, leaving them unaffected, a consequence of their limited extent in space. A smooth transition to the typical form of the matrix in the continuum area occurs at the higher bound states, which reach the absorbing boundary. For the parameters used, the system has 16 bound states, compatible with what is shown in Fig. 1.

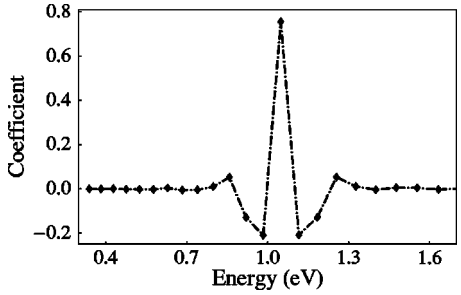

FIG. 2. Part of the state vector of the atom after applying once the AB's linear transformation B on an eigenstate with amplitude 1, with energy approximately 1.1 eV. Dots point to the discrete eigenstates of the atom; the dashed line is used only to help visualization.

A final remark concerning the general form of the matrix: Parallel to the diagonal there appear "satellite" lines, whose magnitude increases for the last eigenstates of the system. We attribute this to the deficiency of the last eigenstates in representing faithfully continuum eigenstates of the system (the density of B-splines is not high enough to describe them). The same is visible, to a smaller extent though, for the first continuum states but of a different origin. Due to the large wavelength, the boundaries affect the eigenstates. The other way around, an inspection of the matrix can reveal the problematic areas.

To test the efficiency of the method, we compared the ionization yield and harmonic generation using a pulse strong and long enough, so that the reflected part of the wave function influences the dynamics [i.e., 1.5 eV $\sin^2$ pulse of 20 cycles (total duration) at an intensity of 2×10^{13} W/cm^2], in a box of $R=400$ a.u. with and without the AB's and in a larger box ($R=800$ a.u.) where the reflection (if present) does not influence the results. We found that the use of AB's provided practically identical results with the larger box, for both physical quantities.

More interesting probably are our results on the PES. In Fig. 3, we present the PES spectra calculated for the hydrogen atom exposed in a laser pulse of $\sin^2$ shape, photon energy 1.5 eV, total duration of 10 cycles, and maximum intensity 4×10^{13} W/cm^2. In (A), we used AB's in a box of $R=400$ a.u. and the PES obtained shows a decrease for photoelectron energies higher than 5 eV due to the absorption of fast electrons at the boundaries. All structure in this spectrum is lost for energies higher than 10 eV. In the same figure, we show the spectrum of the absorbed photoelectrons, which is very small for low energy electrons (not enough velocity to reach the boundary and be absorbed). For a region of energies it is comparable to the population of the electrons not absorbed, and for higher energies it dominates completely. Adding together the populations of the remained and absorbed photoelectrons, we obtain the PES of part (B). We compare this corrected PES with PES obtained in calculations without the use of AB's. In (C) we used the same box size, and we see that the spectra are in perfect agreement up to about 10 eV. In this energy, the ratio of the retained to absorbed population is about 1/10. For higher energies they differ, and the PES calculated without AB's loses the typical structure of successive peaks differing by a photon energy.

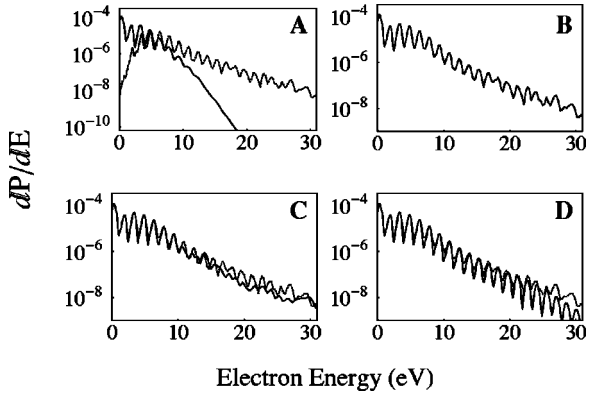

FIG. 3. Common parameters for all plots: A laser pulse of $\sin^2$ shape, photon energy 1.5 eV, total duration of ten cycles, and maximum intensity 4×10^{13} W/cm^2. (A). Photoelectron spectra calculated in a box of $R=400$ a.u. using AB's (solid line). The remaining PES together with the spectrum of the absorbed electrons is given (dashed line). (B). Corrected PES, calculated by adding the retained photoelectron spectra with the absorbed. (C). Comparison of the corrected PES (dashed line) with the PES calculated in a same box (i.e., same eigenstate basis) but without use of AB's (solid line). (D). Comparison of the corrected PES (dashed line) with the PES calculated in a larger box of $R=800$ a.u. (solid line).

The latter is of course due to the reflection of the faster electrons by the boundaries and their artificial reinteraction with the nucleus.

To compare the extended part of the corrected PES, we calculated the PES for a larger box—namely, $R=800$ a.u.. The results are shown in part (D) of the figure. The PES spectra are in good agreement for photoelectron energies up to 20 eV, above which they start to have an important difference. Since we used fixed boundary conditions in the construction of the eigenstates, the density of eigenstates in the continuum drops fast with energy (actually energy goes approximately as j^2, with j the discrete eigenstate index). The distance between two successive peaks in the PES is the photon energy. If in this energy region there are not enough discrete eigenstates, the spectrum is not described well. AB's work in this case as well, but the reconstruction of the PES is not satisfactory. In our example, the level spacing at 20 eV is 0.26 eV, which means that we have about six levels per photon energy, a rather low density.

3. Summary of Sec. II

We presented the construction of a linear transformation on the state vector of an atomic system, equivalent to the AB's employed in the direct solution of the Schrödinger equation on a lattice. The algorithm to construct this transformation is simple, involving standard matrix manipulation. The results enable one to perform time-dependent calculations on a smaller basis, using thus smaller computational resources both in time and space. We illustrated the use of this technique in the case of the hydrogen atom. The harmonic spectrum of the atom calculated is free of artifacts due to reflection and the ionization yields were practically identical with those obtained by enlarging the basis size until the

results converge. In the case of the PES, one can use the additional information of the populations absorbed during the time propagation to obtain results that compare well with the converged PES.

III. GENERALIZATION

A. Introduction

In the previous sections, AB's were imposed on an atomic system by using information of the form of the eigenstates in space. Stepping back, we can see that the TDSE is solved on the eigenstate basis of the system, so the only quantities, except for the external field, that enter in the solution are the energy levels (which represent both the bound and continuum parts of the spectrum) and the dipole matrix elements between the eigenstates.

It is therefore reasonable to assume that the linear transformation that is equivalent to AB's can be calculated based only on the above input. Physically, the dipole matrix elements are irrelevant to the artificial reflection from the boundaries, since they affect only the amplitude transfer between the eigenstates via the external field and not with the propagation of the free part of the wave packet in space. Concerning the energy levels, the critical parameter is naturally the energy level spacing, which is directly connected to the radius of the sphere (fixed boundary conditions). On the other hand, the energy range depends on where we truncate our basis and one could hardly expect the reflection of a wave packet energy centered around 2 eV to depend upon the discretization in the neighborhood of 10 eV.

Based on the previous intuitive arguments, we can conclude that the only physical quantity that affects the reflections is the spectrum we use to represent the continuum. Indeed, discrete modes with constant energy difference $\Delta\omega$ have a free evolution dynamics with period of $2\pi/\Delta\omega$, the time interval needed to be reflected from both boundaries of the box (Fig. 4). This is true irrespective of the form of the boundary conditions and the space extent of the eigenstates. The reflection is completely determined by $\Delta\omega$. If $\Delta\omega$ is variable, the dynamics are not so simple, but as we show, a simple time rescaling suffices to proceed in the same way. In the following, we illustrated through a simple example that the energy levels suffice to calculate the AB linear transformation.

B. Method

1. Single continuum

We chose a physically transparent system to present our method. We consider a photon trapped inside a perfect cavity in one dimension. This system has the advantage that its eigenfunctions of the electric field amplitude take the simple analytical form

$$E_n = \sqrt{\frac{2}{L}} \sin\left(\frac{n\pi x}{L}\right), \tag{7}$$

satisfying immediately the Maxwell equations and the appropriate boundary conditions $[E_n(0)=E_n(L)=0]$.

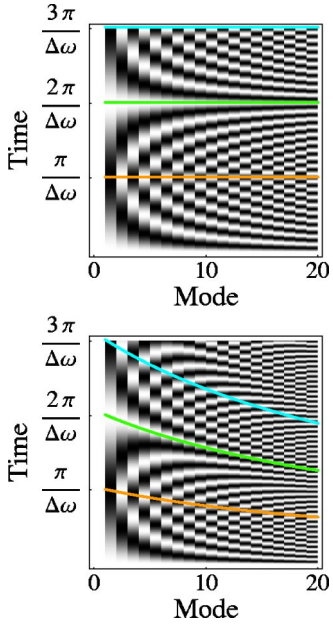

FIG. 4. The real part of the (free) time evolution of the coefficients of an initial state vector $\vec{a}=(1,1,\ldots,1)$ for the first 20 discrete states with constant $\Delta\omega$ (top) and with $\omega(n)=\omega(n-1)+\Delta\omega[1+2a(n-1)]$, $\omega(0)=0$ (bottom). The shading varies from black to white with the state vector element value varying from −1 to +1 and the colored lines show the estimated reflection times for every mode, $t_r(i)$ (see Sec. III B 1 for details). The time interval is long enough to observe the first few reflections at the boundaries (at multiples of $\pi/\Delta\omega$ for constant $\Delta\omega$). Note the reflection symmetry of the top figure with respect to the times of reflection and how the estimated time of reflection (colored curves) matches with the time evolution.

Consider now an initial form of the electric field localized close to zero, the left wall of the cavity. This electric field expressed on the eigenstate basis, truncated so that we deal with the first N modes, would give a state vector (as usually the nth element of the vector stands for the coefficient of the nth eigenstate) that would resemble $\vec{a}_i=(1/\sqrt{N})(1,1,1,\ldots)$.

Keeping in mind the symmetry of the eigenstates with respect to the center of the cavity $(L/2)$ (in the case of even j they are antisymmetric and in the case of odd j they are symmetric) it is straightforward to calculate the coefficients of a wave function being the image of the initial with respect to the center of the well. It would just be $\vec{a}_r=(1/\sqrt{N})(1,-1,1,\ldots)$. This represents practically (letting possible dispersion aside for the time being) the form of the electric field when it is close to the right wall. In Fig. 5 we plot the electric field for the $\vec{a}_i$ coefficients and the reflected $\vec{a}_r$ coefficients.

Due to the simple form of the time evolution of the eigenstates $(c=\hbar=1)$ (top of Fig. 4),

$$E_n(x,t) = \sqrt{\frac{2}{L}} \sin\left(\frac{n\pi x}{L}\right) e^{-i\omega_n t}, \tag{8}$$

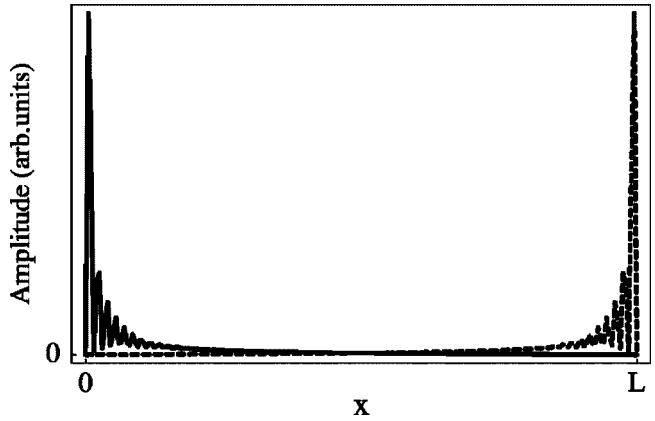

FIG. 5. The electric field for the state vectors $\vec{a}_i$ (heavy line) and $\vec{a}_r$ coefficients (dashed line) for a perfect cavity of length L in arbitrary units. We took into account only the first 150 eigenstates, enough to show the localization of the electric field in space.

$$\omega_n = k_n = \frac{n\pi}{L}, \tag{9}$$

it is easy to estimate the time t_r needed for the electric field to cross the cavity by calculating the necessary time for this sign change. It turns out that $t_r = \pi/\Delta\omega$, where $\Delta\omega = (E_{n+1} - E_n)$ is the discrete energy level spacing. In this case $\Delta\omega = \pi/L$, so $t_r = L$ as expected. In the general case that $\Delta\omega$ is not constant (due to dispersion and/or discretization choice), the reflection time for every ω depends on the local density of states in a way that we discuss in more detail in the following.

We wish to avoid the reflection at the boundary, which is natural for a cavity but not for the open electromagnetic field modeled by the eigenmodes of a cavity. The key idea is that we can project the state vector at any time on a state like the one that is about to be reflected and subtract this part from the initial state vector. This would remove the part of the wave function that is reflected. Of course, AB's should be smooth and have a controllable extent.

It is important to perform this operation without using information about the spatial form of the eigenmodes. This has the following advantages. First, it makes the method flexible and simple, since one needs to know only the energy levels that represent the continuum. Second and more important probably, it circumvents the problem that we mentioned in the previous section—i.e., of evaluating $\mathcal{B}_{nm}$ through Eq. (4) when the box extent is energy dependent. The latter would be a severe limitation, since it limits the class of problems that we can handle to those where the eigenstates are confined in the same box.

To accomplish this, it is sufficient to construct a new basis consisting of N states that correspond to different (ordered) evolution times and gradually remove the last states from the wave function, in accordance with the form of the absorbing boundary we want to use. For illustration reason we show in Fig. 6 few representative states of this type, which we calculated using the eigenstates of Eq. (8). The limited size of the bases causes these states not to be completely localized, having long tails. Nevertheless, this did not cause any problems, since it should affect only the states close to the energy boundaries of the discretized spectrum. Also this is canceled in a large extent because we always have a superposition of modes with a smooth variation of amplitude. Observe, for example, the almost opposite phase of the delocalized oscillation of the new basis states in Fig. 6.

The new basis is constructed as follows. We start by forming a set of vectors describing different evolution times of the system, starting from a initial state close to the origin (at $t=0$), like $\vec{a}_i$, and ending with a state close to the box boundary ($t_r = \pi/\Delta\omega$), like $\vec{a}_r$. Since we want to form a complete basis for N independent modes, we split the time interval into N parts. Using a standard Gram-Schmidt procedure, we take this set of N vectors and generate an orthonormal set of basis vectors.

In brief, the new basis comes from the orthonormalization of a $N \times N$ matrix with elements

$$T_{ij} = \cos\left(\omega_i (j-1)\frac{t_r}{(N-1)}\right), \tag{10}$$

where $\omega_i = (i-1)\Delta\omega$ is the frequency of the ith level with $\omega_1 = 0$ (reference frequency) and $(j-1)t_r/(N-1)$ gives the

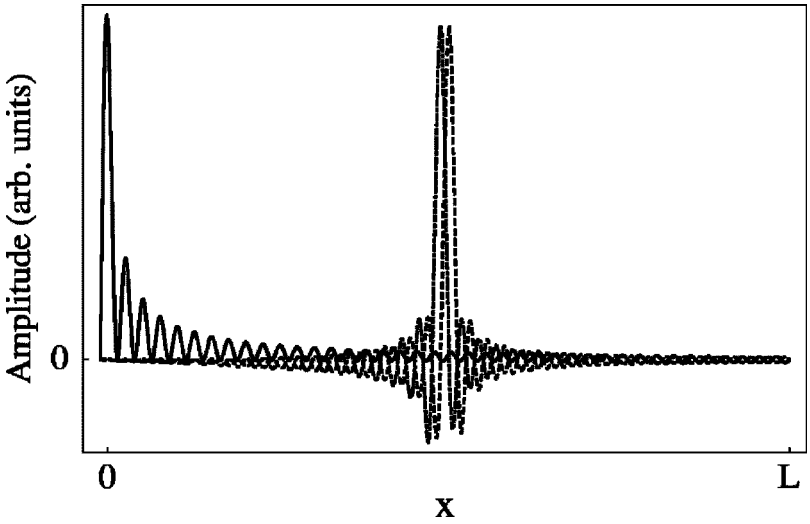

FIG. 6. Few basis states of the new "time evolution" basis used. A basis state at time $t=0$ (solid line) and two consecutive basis states in the middle of the time interval (dot-dashed and dashed lines).

time ranging from 0 to t_r. We used only the real part of the time evolution, so that we deal with a matrix with real elements. This is sufficient, since the transformation is the same for the real and imaginary parts of the state vector.

The matrix must have N independent eigenvectors so that, after orthonormalization, it provides a complete basis for the state vector. This is the case due to the fact that the columns of the matrix are almost orthogonal. The inner product of two rows would be

$$\sum_j T_{mj}T_{nj} = \sum_j \cos\left((m-1)\Delta\omega(j-1)\frac{t_r}{(N-1)}\right) \times\cos\left((n-1)\Delta\omega(j-1)\frac{t_r}{(N-1)}\right) \simeq \int_0^{\pi/\Delta\Omega} \cos[(m-1)\Delta\omega t] \times\cos[(n-1)\Delta\omega t] = \delta_{mn}.$$

The inner product is not exactly zero because it is a finite representation of the integral. This provides confidence that there are indeed N independent eigenvectors and verified by the observation that the changes from the orthonormalization to the vectors (columns) were very small. Then the absorbing boundary matrix is constructed as explained in more detail in the previous section. Since the eigenvectors of this basis is time ordered, the mask now removes gradually the last. Its extent is effectively measured in the number of modes of the new basis it removes.

The main limitation is inevitably encountered at the edge(s) of the discrete energy spectrum due to the lack of neighboring levels, so one has to ascertain that these states do not play a significant role in the phenomenon examined. In that case, an attenuation in time of these states by a simple exponential decay could remove the problem.

The case of dispersion or of free boundary conditions requires a slightly different approach. The reflection time is not the same for all the levels, since $\Delta\omega$ varies. On the contrary, it depends for each level on the density of modes in the vicinity of the corresponding level. This is circumvented by creating a T_{ij} matrix, in which the propagation time [previously just $(j-1)t_r/(N-1)$] is not common for all modes. Instead we use for each level the same fraction of the local reflection time.

The local reflection time is calculated by a simple physical analogy with an equivalent problem. We want to imitate a given discrete spectrum with the spectrum of a, more or less, easily understood system. Consider again the electric field in a one-dimensional cavity with perfectly reflecting boundaries, but now the (right) boundary position depends on frequency, using, for example, a multilayer mirror. This dependence shapes the spectrum (Fig. 7) in a controlled way. Working the other way around, a given spectrum determines the boundary positions (i.e., reflection positions for every frequency), so the effective cavity length L_i for every mode is known and subsequently the reflection time, which is just L_i since $c=1$.

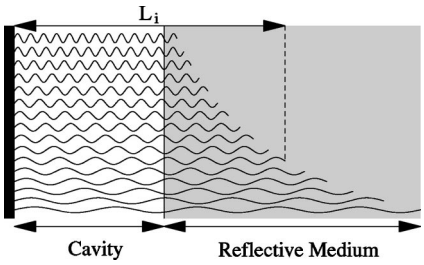

FIG. 7. The equivalent cavity that imitates a given spectrum. The left wall reflects all frequencies at the same point while the right wall reflects every frequency at a different depth. So every mode sees a cavity with different dimensions (L_i) enabling us to shape the spectrum.

We set the frequency of the photon of the first mode $\omega_1 = 0$ as the reference for all frequencies. This mode is not supported by the cavity and we deal with it separately. Then ω_2 is the frequency of the photon of the first mode of the cavity and ω_3 of the second mode and so on. Since now $\omega_i = k_{i-1}$ we have $i\pi/L_i = \omega_{i+1}$, so $L_i = i\pi/\omega_{i+1}$. Thus the reflection time for each mode is $t_r(i) = L_{i-1} = (i-1)\pi/\omega(i)$ with the only parameters being the frequency and index of the mode. The reflection time for the first mode is not important since its time evolution is trivial. Nevertheless, if necessary, one can extrapolate the reflection time for this mode.

The result we obtained from this simple physical analogy was tested for a number of dispersion relations, $\omega \propto k, k^2, k^3$, and it reproduced the correct reflection time we expect. However, we found that this approach fails in the case of a discontinuous derivative of $d\omega/dk$, a case that needs special handling, for example: isolation of the discontinuity by splitting the discrete spectrum in two parts.

In Fig. 4 we show the local reflection time as we calculate it which matches with the free time evolution of the modes. For example, for the first reflection it intersects the time evolution of each mode has an alternating value of ± 1 and for the second reflection all modes have value 1.

So in the case of free boundary conditions or of dispersion, we can use

$$T_{ij} = \cos\left(\omega_i(j-1)\frac{t_r(i)}{(N-1)}\right), \tag{11}$$

with a rescaled time coordinate different for every mode. Effectively, this means that the extent of absorbing boundaries is now mode dependent and covers the same fraction of the mode reflection time.

Besides these intuitive arguments, there exists a simple mathematical approach which should by now be clear. Given a set of N modes we construct a new basis, on which we are able to represent the coefficient vector of the system throughout its time evolution. This basis has to be complete and time ordered and is constructed as we showed. The reflection time is used to make the bases complete and (almost) orthogonal.

2. Multiple continua

In the case of multiple discretized continua, the same method is applicable with minor extensions. For example, assume a double continuum, the eigenstates of which are a product of single continuum eigenstates. For simplicity, consider we use N eigenstates of the first and M eigenstates of the second single continuum. There are $N \times M$ combinations, so the state vector has $N \times M$ elements that form the finite basis of the double continuum. By suitable permutations, the state vector can be ordered like $(c_{11}, c_{12}, c_{13}, \ldots, c_{1m}, c_{21}, c_{22}, \ldots)$. The first M states are composed of the first state of continuum "1" and all the states of continuum "2", the next M are composed by the second state of continuum "1" and all the states of continuum "2" and so on. We construct the absorbing boundary matrix for the first block of M states using their energy levels; then for the following blocks of M states it is the same since it depends only on the spacing of the energy levels and not on their value. Then the complete absorbing boundary matrix for continuum "2" is a block diagonal consisting of the previous matrix. Then we employ another set of permutations to order the state vector like $(c_{11}, c_{21}, c_{31}, \ldots, c_{n1}, c_{21}, c_{22}, \ldots)$ and construct in the same way the block diagonal absorbing boundary matrix for the continuum "1". The complete transformation can thus be included in a matrix being the product of the above transformations, with a general form

$$\mathcal{B}_d = P_1^{-1} \mathcal{B}_1 P_1 P_2^{-1} \mathcal{B}_2 P_2, \tag{12}$$

where $P_{1,2}$ is a suitable permutation matrix used to reorder the state vector as described, $\mathcal{B}_{1,2}$ is the block-diagonal absorbing boundary matrix for continuum "1" or "2."

Consider now the simple case of a double continuum, which is composed of a small number of single-continuum eigenstates. For example, the eigenstates of a free electron in two dimensions are the product of the eigenstates of the electron in the x and y directions. Limiting the system to a rectangle and taking 30 eigenstates in both single continua would result in $30 \times 30 = 900$ double-continuum eigenstates. For simplicity we choose the eigenstates to have constant energy difference; thus, the spectrum consists of equally spaced energy levels.

Ordering the state vector in a way that the first permutation is useless, we proceed with the construction of the single-continuum absorbing boundary matrix $\mathcal{B}_{1,2}$ and then of the double-continuum matrix $\mathcal{B}_d$ which is shown in Fig. 8. Because of the simple ordering of the state vector we chose, there is a similarity of the structure of the $\mathcal{B}_d$ matrix with its single-continuum analog. In addition, it becomes clear how this transformation actually works, by combining eigenstates within a block (i.e., with one continuum eigenstate common) and at the same time combining neighboring blocks in an analog way (satellites of the diagonal of the matrix).

In practice, since the size of the matrix for the transformation increases very fast, $(N \times M)^2$, we can avoid constructing such a big matrix by repeatedly applying the single-continumm absorbing matrices on the appropriate part of the state vector every time and replacing immediately their values. One point worth noting in this case is that since the transformation we perform is sensitive to the relative phase of the coefficients, we have to be careful to apply the transformed ordered, e.g., for the first continuum and afterwards for the second. So in this way we have M applications of a N^2 matrix followed by N applications of a M^2 matrix.

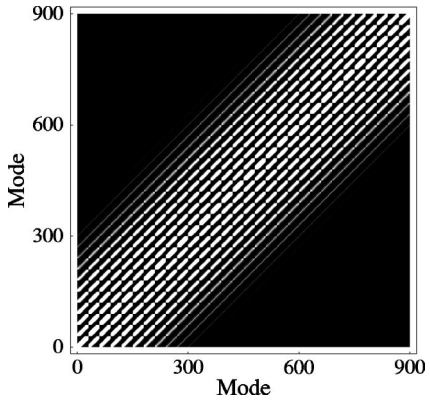

FIG. 8. Double continuum AB matrix. The shading varies from black to white with increasing absolute value of the matrix elements. The structure of the matrix shows how the eigenstates are mixed to imitate AB's and at the same time the limitations due to the finite bases (see text for details).

3. Constructing differential equations with inherent AB's

So far, the application of AB's has been accomplished by a linear transformation on the state vector of the system in specific times during the propagation of the differential equations. We have found that it is also possible to add a term in the differential equation for every mode belonging to a discretized continuum, so that the system of differential equation inherently contains AB's.

The differential equation for the amplitude of a discrete mode belonging to a single continuum looks like

$$i\dot{b}_i = \omega_i b_i + CT, \tag{13}$$

where the term $\omega_i b_i$ is the free evolution of the mode and CT stands for all the coupling terms that represent the interaction of this mode with the rest of the system. We add a term which causes attenuation to the "part" of the amplitude that approaches the boundaries.

In brief, consider the matrix $\tilde{\mathcal{B}} = \mathcal{I} - \mathcal{B}$. This matrix performs the opposite transformation compared to $\mathcal{B}$. It removes the part of the wave function (or electric field) close to the origin and keeps the part that is close to the boundaries, with the same width as the mask. The latter is the part we want to remove, so we add to the differential equation a term which leads to an exponential decay of the amplitude of the mode, when the wave function is approaching the boundary. We also introduce a damping constant γ so that we have control over the decay rate. The later is directly related to the width of the AB's, so that there is enough time for (almost) complete attenuation of the wave function. The modified differential equation reads

$$i\dot{b}_i = \omega_i b_i + CT - i\gamma \sum_{j=1}^{N} \tilde{\mathcal{B}}_{ij} b_j, \tag{14}$$

where the last term is our addition. When the wave function is close to the beginning, this term is practically zero and does not influence the dynamics of the system. Once there is a part of the wave function approaching the boundary, this term takes significant values and causes an attenuation of the amplitude, but in a controlled way, so that only the part of the wave function approaching the boundaries is removed. In the next section, we apply this idea to the physically transparent problem of spontaneous emission.

C. Applications

1. Spontaneous emission

We consider a TLA with ground ($|g\rangle$) and excited ($|e\rangle$) states with energy difference ω_0 ($\hbar=0$). The atom is initially in the excited state and is coupled with the continuum of the modes of the electromagnetic field in free space. This problem can be handled analytically, because of the simple structure of the coupling, leading to the well-known exponential decay of the excited state. We use this simple problem to illustrate the usefulness of AB's.

The Hamiltonian of the system in the interaction picture and in the rotating-wave approximation is

$$H = \omega_0 \sigma_{ee} + \sum_{\lambda} \omega_\lambda \alpha_\lambda^\dagger \alpha_\lambda + \sum_{\lambda} g_j (\alpha_\lambda \sigma^+ + \alpha_\lambda^\dagger \sigma^-), \tag{15}$$

where $\sigma^+ = |g\rangle\langle e|$ and $\sigma^- = |e\rangle\langle g|$ are the atomic raising and lowering operators, and $\sigma_{ee} = \sigma^+\sigma^-$. The field operators $\alpha_\lambda^\dagger, \alpha_\lambda$ correspond to the modes of the free electromagnetic field which are coupled to the atom via the respective coupling constant g_λ. In this Hamiltonian we have replaced the true continuum of the modes of the electromagnetic field by a collection of discrete modes.

In this approximation, the wave function for the full system reads

$$|\psi\rangle = \alpha_0 |e,0\rangle + \sum_{\lambda} b_\lambda |g,1_\lambda\rangle, \tag{16}$$

where the amplitudes b_λ correspond to the discrete modes of the electromagnetic field and α_0 is the amplitude of the excited state of the two-level atom.

The time evolution of the amplitudes is governed by the Schrödinger equation, from which we obtain

$$i\dot{a}_0 = \omega_0 a_0 + \sum_{\lambda=1}^{N} g_\lambda b_\lambda, \tag{17}$$

$$i\dot{b}_\lambda = \omega_\lambda b_\lambda + g_\lambda a_0. \tag{18}$$

One has to choose a range of frequencies (ω_l, ω_u) of the electromagnetic field and discretize this frequency range. In our simple example we chose $\omega_l = \omega_0/2$ and $\omega_u = 3\omega_0/2$, with $\omega_0 = 1$, and used N equidistant modes inside this frequency range and a constant coupling g_λ. For the latter we used a value of $g_\lambda = 0.03/\sqrt{N}$ so that the decay rate is independent of the number of modes.

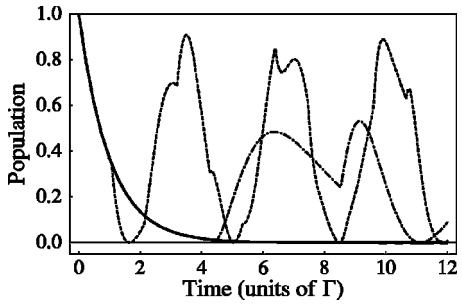

FIG. 9. Population of the excited state of the two-level atom as a function of time. For the dashed and dot-dashed curves, $N=30$ and $N=120$, respectively. The solid curve is calculated with $N=30$, but with the use of AB's. The analytic solution coincides with the later with deviations of at most 0.5% for time $\Gamma t=12$).

We calculated the population of the excited state as a function of time using $N=30$ and $N=120$ discrete modes without AB's (Fig. 9). The artifacts of the calculation (revivals) due to the reflection of the emitted photon by the boundaries are apparent for both cases. Together we show the result with $N=30$ discrete modes, but this time with the use of AB's. It is evident in this case that these artifacts are removed. For a more quantitative test, we used the analytic solution for the population of the excited state. The exponential decay we expect has to be corrected to account for two things. First, the short-time behavior is not exponential, so we have to perform a small time shift and, second, the exponent is slightly modified ($\sim 3\times 10^{-3}$) due to the limited frequency range we considered. Taking those two effects into account, our result differs from the analytic one by at most 0.5% at $\Gamma t=12$.

Switching now to the different approach we discussed in the last part of the previous section, we modify the differential equations we solve in such a way that they include AB's. For this case, the new system of equations reads

$$i\dot{a}_0 = \omega_0 a_0 + \sum_{\lambda=1}^{N} g_\lambda b_\lambda, \tag{19}$$

$$i\dot{b}_\lambda = \omega_\lambda b_\lambda + g_\lambda a_0 - i\gamma \sum_{\mu=1}^{N} \tilde{\mathcal{B}}_{\lambda\mu} b_\mu, \tag{20}$$

where the first equation remains the same since it represent a true discrete state.

In Fig. 10 we show again the population of the excited state as a function of time calculated using $N=30$ discrete modes and a depth of AB's of ten modes (full width at half maximum), employing the modified differential equations. For γ as small as 10^{-3} there is not enough time to absorb the electric field that approaches the boundary, so we still have artifacts due to the reflection, but less pronounced compared to the case of no AB's. Increasing γ to 10^{-2} leads to results apparently free from reflections.

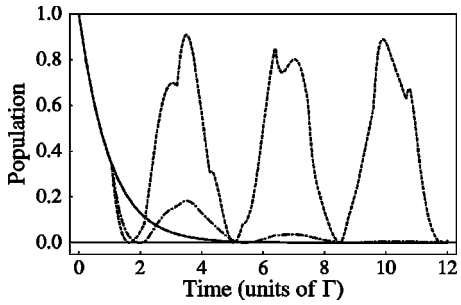

FIG. 10. Population of the excited state of the TLA as a function of time for different values of the damping in the modified differential equations. The damping constant γ is 0, 10^{-2}, and 10^{-1} for the dashed, dot-dashed, and solid curves respectively. We used $N=30$ discrete modes in all cases.

A more detailed comparison is shown in Fig. 11 where we show the ratio of our numerical calculations over the analytic result. In the case γ is small, the deviations are larger, but for reasonable values of γ the results are practically identical to the analytic solution for values of time up to $\Gamma t=12$.

2. TLA and two photons

In this part we compare our results with previously published ones [18], on a more complicated problem, involving the interaction of two photons with a TLA and a defect mode. The computational difficulties of problems involving multiple continua—i.e., in this case the number of differential equations scaling roughly as N^2 with the number of the discrete modes necessary to describe the single continuum—are a fertile playground for illustrating the capabilities of our method.

A TLA is coupled to a PBG, which is modeled by a set of discrete modes. The atom is also coupled to a defect mode inside the gap which acts as a photon source that can pump the atom. We follow the lines of [18] in the description of this system.

In brief, we consider a TLA as in the previous part, only this time the Hamiltonian due to the coupling with the defect mode reads

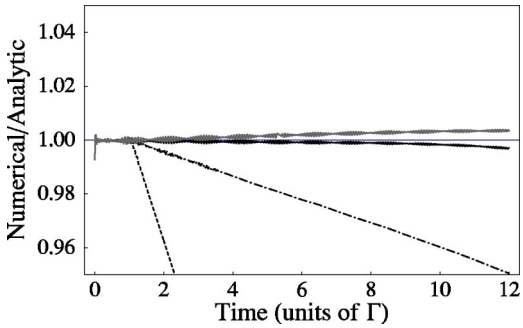

FIG. 11. The ratio of the numerical over the analytic solution for the decay of the excited state of the TLA as a function of time for different values of the damping in the modified differential equations. The damping constant γ is 0.1, 0.15, 1, and 10 for the dashed, dot-dashed, solid black, and solid gray curves, respectively.

$$H=\omega_0\sigma_{ee}+\omega_d\alpha_d^\dagger\alpha_d+\sum_\lambda\omega_\lambda\alpha_\lambda^\dagger\alpha_\lambda+g_d(\alpha_d\sigma^+ +\alpha_d^\dagger\sigma^-)$$
$$+\sum_\lambda g_\lambda(\alpha_\lambda\sigma^+ +\alpha_\lambda^\dagger\sigma^-). \tag{21}$$

The field operators $(\alpha_d,\alpha_d^\dagger)$ and $(\alpha_\lambda,\alpha_\lambda^\dagger)$ correspond to the defect mode and the PBG reservoir, respectively, which are coupled to the atom via the respective coupling constants g_d and g_λ.

We consider the case where the defect mode is initialy prepared in the one-photon Fock state $(n=1)$ and the TLA in the excited state. So we have a total of two excitations and, thus, the state vector of the system reads

$$|\psi(1,t)\rangle=\alpha_0|e;1_d,0\rangle+b_0|g;2_d,0\rangle+\sum_\lambda b_\lambda|g;1_d,1_\lambda\rangle$$
$$+\sum_\lambda a_\lambda|e;0_d,1_\lambda\rangle+\sum_{\substack{\lambda,\mu\\ \lambda\geqslant\mu}} b_{\lambda\mu}|g;0_d,1_\lambda\rangle, \tag{22}$$

where $b_{\lambda\mu}=b_{\mu\lambda}$ and initially $|\psi(1,0)\rangle=|e;1_d,0\rangle$.

In the context of an isotropic model, the spectral response $D_I(\omega)$ for the PBG continuum is given by

$$D_I(\omega)=\frac{C}{\pi}\frac{\Theta(\omega-\omega_e)}{\sqrt{\omega-\omega_e}}, \tag{23}$$

where C is the effective coupling of the atomic transition to the structured continuum, Θ the step function, and ω_e the band-edge frequency. We follow the discretization technique as explained in more detail in [18]. The density of states (DOS) in the frequency range important for the system (ω_l,ω_u) is replaced by a number of discrete modes inside this frequency range. In our problem, $\omega_l=\omega_e$, due to the step function limitation, and $\omega_u=10C^{2/3}$ as chosen in [18]. We can use for the frequencies of the discrete modes [18,19]

$$\omega_j=\omega_e+j^2\delta\omega, \tag{24}$$

with a common atom-field coupling constant for all modes:

$$g_r\simeq\sqrt{\frac{2C}{\pi}\sqrt{\delta\omega}}. \tag{25}$$

The time dependence of the amplitudes is governed by the Schrödinger equation, and after the elimination of the off-resonant part of the continuum $(\omega>\omega_u)$ we find [20]

$$i\dot{a}_0=(\Delta_0+\Delta_d-S)a_0+\sqrt{2}g_d b_0+\sum_{j=1}^{N}g_j b_j, \tag{26}$$

$$i\dot{b}_0=2\Delta_d b_0+\sqrt{2}g_d a_0, \tag{27}$$

$$i\dot{a}_j=(\Delta_0+\Delta_j-S)a_j+g_d b_j+\sum_{k=1,k\neq j}^{N}g_k b_{jk}+\sqrt{2}g_j b_{jj}, \tag{28}$$

$$i\dot{b}_j=(\Delta_j+\Delta_d)b_j+g_j a_0+g_d a_j, \tag{29}$$

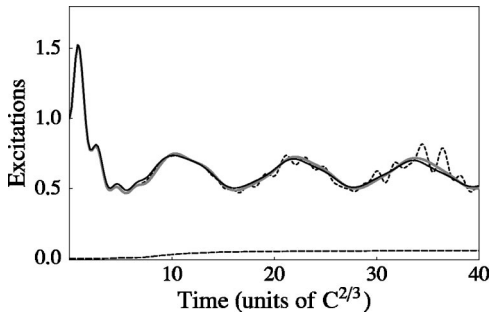

FIG. 12. The mean photon number in the defect mode calculated using $N=30,150$ modes (dashed and solid curves) and $N=30$ with AB's (gray solid curve). We also show the absorbed part of the wave function corresponding to the mean photon number in the defect mode (lower dashed curve), which we added to the remaining part of the wave function to obtain the gray solid curve. Parameters are as in [18]—i.e., $\omega_u=10C^{2/3}$, $\Delta_0=\Delta_d=-0.1C^{2/3}$, and $g_d=1.0C^{2/3}$.

$$i\dot{b}_{jk}=(\Delta_j+\Delta_k)b_{jk}+g_k a_j+g_j a_k, \tag{30}$$

$$i\dot{b}_{jj}=2\Delta_j b_{jj}+\sqrt{2}g_j a_j, \tag{31}$$

where j,k are the indices of the N discrete modes and $g_j=g_k=g_r$, while $\Delta_0=\omega_0-\omega_e$, $\Delta_d=\omega_d-\omega_e$, and $\Delta_j=\omega_j-\omega_e$. The shift term is given by

$$S=\sum_{\substack{\mu \\ \mu>N}}\frac{g_\mu^2}{\omega_\mu-\omega_e}, \tag{32}$$

where N is the number of discrete modes we use.

In Fig. 12 we show our results for the time evolution of the mean photon number in the defect mode (same as Fig. 2 in [19]). We performed the same calculations for $N_n=30,150$ and with $N_{ab}=30$ using AB's. The revivals of the population for the case $N_n=30$ are evident and they appear as early as $\Gamma t=13$. Using $N_n=150$ we are free from revivals up to $\Gamma t=40$ and this represents the converged result in this time range [18]. Employing now AB's and using $N_{ab}=30$ modes we obtain results that compare well with the latter. In analogy with our first example, the reconstruction of the PES of an atom, we kept track during the propagation of the population changes due to the absorption and we added it to the remaining population to obtain our final result as presented.

Regarding computational cost, we had to solve about $(f=N_n/N_{ab})^2=25$ times fewer equations, although we have to perform in the meantime the neccesarry transformations. This is an important improvement, and already for the double continuum it shows the potential of our method. Consider that the improvement (in the number of equations necessary) scales as f^m where m is the multiplicity of the continuum and f ratio of the necessary modes with AB's over the necessary modes without.

IV. SUMMARY

We have shown that it is possible to apply AB's on the time propagation of the Schrödinger equation for a real atomic system on the basis of its field-free eigenstates by using a simple linear transformation. This means that the artificial reflection of the wave packet at the boundaries is remedied, so the calculations can be performed on a smaller basis (in space extent) and thus faster. Also, since information about which part of the wave function (energy resolved) is removed or modified during the time propagation is easily available, one can use this additional information to reconstruct the final state of the atom (regarding populations, not amplitudes, since phase information is lost), in the case that nothing was absorbed or reflected. One should note, though, that in the case of a low density of states in the continuum, the continuum is not represented accurately from the beginning. In this case AB's do remove artifacts due to reflections, but the reconstruction of sensitive quantities (like the PES) is not more succesfull than the basis allows.

More important probably, a generalization of this method has been proposed to handle the general problem of a discretized energy continuum, based only on the energy spectrum used to approximate the continua. The calculation of the linear transformation can be accomplished numerically or even analytically in simple cases and is performed through standard linear algebra operations. We have also shown how to generalize this method to multiple continua, examining in detail the case of a double continuum. We have further proposed an alternative approach, in which the AB's are incorporated into the (modified) system of differential equations one has to solve.

We thus applied our method to two systems, the spontaneous emission of a TLA in free space and the interaction of a TLA, a defect mode, and two photons at the adge of a PBG. In the first case, our result practically coincides with the analytic one, illustrating our method in this simple physical system. The second case we examined is more complicated, since we chose to deal with two photons, meaning that the number of the necessary modes is much larger. We compared our results with previously published ones [19] and demonstrated a computational improvement of more than an order of magnitude.

The application range of this method covers all time-dependent problems solved by energy discretization (for example two-electron atoms [17], atom lasers [21–25], quantum electrodynamics with few photons [18–20]), without modifications. The computational benefit turns out to be significant and scales as the power of the continuum multiplicity.

ACKNOWLEDGMENTS

I would like to thank P. Lambropoulos for his thorough critical reading of the manuscript, G. M. Nikolopoulos for his help on the two-photon problem, and S. I. Themelis for drawing my attention to complex rotation methods. This work was supported by the ΗΡΑΚΛΕΙΤΟΣ program of ΕΠΕΑΕΚ II, funded by the Greek Ministry of Education and the European Union.

[1] X. Tang, H. Rudolph, and P. Lambropoulos, Phys. Rev. Lett. **65**, 3269 (1990).
[2] K. C. Kulander, Phys. Rev. A **35**, 445 (1987).
[3] J. L. Krause, K. J. Schafer, and K. C. Kulander, Phys. Rev. A **45**, 4998 (1992).
[4] W. P. Reinhardt, Annu. Rev. Phys. Chem. **33**, 223 (1982).
[5] Y. K. Ho, Phys. Rep. **99**, 1 (1983).
[6] S. D. Parker and C. W. McCurdy, Chem. Phys. Lett. **156**, 483 (1989).
[7] C. W. McCurdy and C. Stroud, Comput. Phys. Commun. **63**, 323 (1991).
[8] M. Pont, D. Proulx, and R. Shakeshaft, Phys. Rev. A **44**, 4486 (1991).
[9] B. Piraux and R. Shakeshaft, Phys. Rev. A **49**, 3903 (1994).
[10] U. V. Riss and H.-D. Meyer, J. Phys. B **31**, 2279 (1998).
[11] T. Grosges, B. Piraux, and H. Bachau, Phys. Rev. A **60**, 1371 (1999).
[12] A. M. Ermolaev, I. V. Puzynin, A. V. Selin, and S. I. Vinitsky, Phys. Rev. A **60**, 4831 (1999).
[13] S. Yoshida, S. Watanabe, C. O . Reinhold, and J. Burgdörfer, Phys. Rev. A **60**, 1113 (1999).
[14] M. Makris, Ph.D. thesis, University of Crete, 2003.
[15] T. Chang, *Many-Body Theory of Atomic Structure* (World Scientific, Singapore, 1993).
[16] J. Sapirstein and W. Johnson, J. Phys. B **29**, 5213 (1996).
[17] P. Lambropoulos, P. Maragakis, and J. Zhang, Phys. Rep. **305**, 203 (1998).
[18] G. M. Nikolopoulos and P. Lambropoulos, J. Opt. Soc. Am. B **3**, 115 (2001).
[19] G. M. Nikolopoulos and P. Lambropoulos, Phys. Rev. A **61**, 053812 (2000).
[20] G. M. Nikolopoulos, S. Bay, and P. Lambropoulos, Phys. Rev. A **60**, 5079 (1999).
[21] J. J. Hope, Phys. Rev. A **55**, R2531 (1997).
[22] G. M. Moy and C. Savage, Phys. Rev. A **56**, R1087 (1997).
[23] G. M. Moy, J. J. Hope, and C. Savage, Phys. Rev. A **59**, 667 (1999).
[24] J. J. Hope, G. M. Moy, J. M. Collet, and C. Savage, Phys. Rev. A **61**, 023603 (2000).
[25] G. M. Nikolopoulos, P. Lambropoulos, and N. P. Proukakis, J. Phys. B **36**, 2797 (2003).